JCTC Journal of Chemical Theory and Computation

Article

pubs.acs.org/JCTC

Role of the Membrane Dipole Potential for Proton Transport in Gramicidin A Embedded in a DMPC Bilayer

Jens Dreyer,[†,‡] Chao Zhang,[†,‡,#] Emiliano Ippoliti,[†,‡] and Paolo Carloni*[,†,‡]

[†]Computational Biophysics, German Research School for Simulation Sciences, Joint venture of RWTH Aachen University and Forschungszentrum Jülich, Germany, D-52425 Jülich, Germany

[‡]IAS-5, Computational Biomedicine, Institute for Advanced Simulation, Forschungszentrum Jülich, D-52425 Jülich, Germany

Supporting Information

ABSTRACT: The membrane potential at the water/phospholipid interfaces may play a key role for proton conduction of gramicidin A (gA). Here we address this issue by Density Functional Theory-based molecular dynamics and metadynamics simulations. The calculations, performed on gA embedded in a solvated 1,2-dimyristoyl-*sn*-glycero-3-phosphocholine (DMPC) model membrane environment (about 2,000 atoms), indicate that (i) the membrane dipole potential rises at the channel mouth by ∼0.4 V. A similar value has been measured for gA embedded in a DMPC monolayer; (ii) the calculated free energy barrier is located at the channel entrance, consistent with experiments comparing gA proton conduction in different bilayers. The electronic structures of the proton ligands (water molecules and peptide units) are similar to those in the bulk solvent. Based on these results, we suggest an important role of the membrane dipole potential for the free energy barrier of proton permeation of gA. This may provide a rationale for the large increase in the rate of proton conduction under application of a transmembrane voltage, as observed experimentally. Our calculations might suggest also a role for proton desolvation for the permeation process. This role has already emerged from EVB calculations on gA embedded in a model membrane.

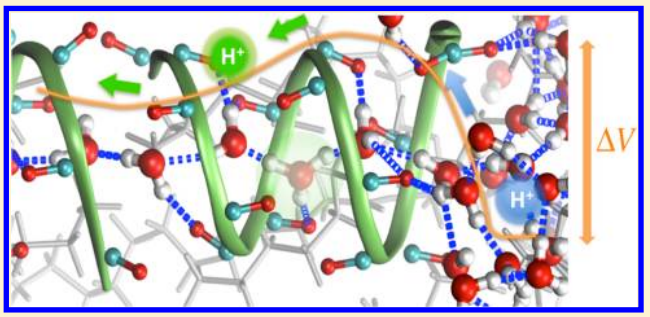

INTRODUCTION

The cation-selective membrane channel gramicidin A (gA) is a widely used antibiotic against gram-positive bacteria.[1] Its beneficial properties are due to its ability to trigger the efflux of potassium ions from inside the host cells[2] and/or by acidifying the bacterial cytoplasm.[3−5] Particularly prominent is gA's efficiency in conducting protons.[6] In spite of the low relevance of tunneling effects,[7,8] gA permeates H^+ ions at a faster rate than any other membrane channel. Indeed the measured rate is up to 2×10^9 H^+ s^{-1} under a transmembrane potential of 0.16 V.[6] The effect of the membrane potential is dramatic: proton conduction in gA decreases hundreds of times without external potential.[6] This performance is reached by a simple architecture: two pentadecapeptides with alternating D- and L-amino acid residues forming a β-helix pore of about 3 Å diameter, with the peptide carbonyl groups aligned along the channel pore.[9] The experimentally measured, nearly direct proportionality between proton current and proton concentration in gA from pH 4.5 to pH −0.5 with external voltage has led to the suggestion that the energy barrier is present at the channel mouth.[10−12]

Investigating the membrane potential experienced by the proton on passing from the bulk solvent to gA's interior is important for elucidating the mechanism of proton permeation through ion channels, including gA.[10,13−15] This membrane potential is made up of several contributions: (i) A large positive potential, referred to as the membrane dipole potential (ΔV_{DP} hereafter).[13,16] This is present in the region between the aqueous phase and the hydrocarbon-like interior of the membrane. ΔV_{DP} is attributed to the alignment of the dipolar residues of the lipids and the partial alignment of water molecules at the membrane/solvent interface.[13,17,18] The contributions of polarized water and of the polar lipid head groups are indistinguishable in most experiments.[18−20] Hence, ΔV_{DP} reflects the electrostatic potential difference at the dielectric mismatched membrane and water regions.[21] (ii) The surface potential (ΔV_S) generated by ions adsorbed on the lipid head groups present at the membrane/water interface. Obviously, ΔV_S depends strongly on the ionic strength. (iii) An additional contribution referred to as transmembrane potential arises from the charge imbalance that is generated if the ion concentration in the extracellular and intracellular side of the channel differ.

The role of ΔV_{DP} for gA's proton permeation has been investigated both experimentally and computationally. Experimentally, conductances G_{H^+} and ΔV_{DP} have been reported for gA embedded in the glycerol 1-monooleate (GMO), diphytanoylphosphatidylcholine (DPhPC), dipalmitoylphosphatidylcholine (DPPC), and dioleoylphosphatidylcholine

Received: May 7, 2013
Published: July 9, 2013

(DOPC) membrane bilayers, at different H^+ bulk concentrations (Table 1). Unfortunately, at present there are no general and conclusive arguments on the role of ΔV_{DP} for the proton conductance.[10,13−15] Indeed, in going from GMO to DPhPC, i.e. from a membrane with polar head groups to one with zwitterionic head groups and strongly increasing ΔV_{DP}, G_{H^+} increases only slightly at low H^+ bulk concentration (0.1 M). On the other hand, at very high H^+ bulk concentration (1.0 M) G_{H^+} is larger in GMO than in DPhPc (Table 1).[22] At this concentration G_{H^+} in DPPC was measured to be smaller than in DPhPC, while ΔV_{DP} is larger in DPPC than in DPhPC. G_{H^+} is similar in DPPC and DOPC, whereby ΔV_{DP} is somewhat smaller for DPPC than for DOPC.[19] The latter has been measured though with a different technique as compared to the other membranes reported in Table 1. When G_{H^+} is evaluated against the local membrane/water interface H^+ concentration instead of bulk concentration, the conductance is almost a factor of 10 lower in GMO than in DPhPC.[15] Deviating results for the few cases measured so far reflect the considerable influence of different experimental conditions on G_{H^+} and ΔV_{DP} (Table 1).

Table 1. Single Channel Proton Conductances (G_{H^+}) and Membrane Dipole Potentials (ΔV_{DP}) Measured for gA at Room Conditions

membrane	$[H^+]_{bulk}$ [M]	G_{H^+} [pS]	ΔV_{DP} [V]
GMO	0.1	∼190[a]	0.100 ± 0.009[c]
	1.0	∼1000[a]	0.100 ± 0.009[c]
DPhPC	0.1	∼200[a]	0.228 ± 0.005[c]
	1.0	789 ± 12[a,b]	0.228 ± 0.005[c]
DPPC	1.0	664 ± 38[a,b]	0.243 ± 0.004[c]
DOPC	1.0	660 ± 9[a,b]	0.275[d]

[a]Measurement of single SS dioxolane-linked gA channels.[15,23] Bilayers were formed from a 0.06 M solution of lipids in *n*-decane; 1−3 gA channels were incorporated into the bilayer.[24] [b]Reference 12. [c]Measurements of bilayers using the charge relaxation method;[18] membranes were prepared from 20 mg lipid/ml *n*-decane in a buffer of 0.02 M 4-morpholine ethanesulfonic acid and 0.05 M (DPhPC) or 0.1 M KCl (GMO) at pH 5.5. [d]Measured by atomic force microscopy;[19] membranes were prepared in ∼0.0005 M NaCl solution.

At the computational level, ΔV_{DP} has been reported by a semiempirical study (MS-EVB) on proton permeation for the gA channel embedded in GMO and DPhPC.[25] This study calculated rate-limiting free energy barriers for proton permeation ($\Delta G^{\#}$) comparable with those of experiments (Table S1). It was proposed that ΔV_{DP} does not account for differences in the barrier heights for proton permeation in gA embedded in the two membranes reported in Table 1.[25] However, induced polarization effects − lacking in these semiempirical approaches − have been suggested to be an indispensable ingredient of ΔV_{DP}.[16] This calls for further computational investigations to address the role of ΔV_{DP} for proton permeation.

Ab initio Car−Parrinello molecular dynamics (CPMD) simulations[26] have emerged as a useful tool for investigating proton transfer in aqueous solutions, in narrow pores and at membrane interfaces.[27−37] This approach, which is based on electronic structure calculations using density functional theory (DFT), includes electronic polarization, allowing one to properly investigate the role of ΔV_{DP} for proton permeation in gA. Previously, proton migration in biological systems such as aquaporins[38] or bacteriorhodopsin[39,40] has been described by hybrid quantum mechanics/molecular mechanics CPMD[41] approaches. Currently, Tier-0 supercomputing initiatives such as INCITE (http://www.doeleadershipcomputing.org) in the US or PRACE (http://www.prace-project.eu/) in the EU allow the investigation of entire ab initio systems of thousands of atoms and with time scales of several tens of picoseconds. The availability of such resources has prompted us to investigate the role of ΔV_{DP} for the proton permeation process in gA from an ab initio perspective.

COMPUTATIONAL DETAILS

Our system consists of the gA dimer, 8 1,2-dimyristoyl-*sn*-glycero-3-phosphocholine (DMPC) lipid membrane molecules, 138 water molecules and one excess proton with a box size of 22.6 × 19.6 × 39.9 Å^3 applying periodic boundary conditions (1911 atoms in total, see Supporting Information, Figure S1). It was prepared by using classical MD simulations based on a solid state NMR structure.[42] It features the same ratio between gA and DMPC as in the NMR experiments.[42] It also includes the interaction between gA's 8 Trp residues and the lipid environment, which affect gA's stability and conductance.[43,44]

The electronic structure problem was solved within the framework of DFT using the BLYP gradient-corrected functional as implemented in the CPMD 3.13.2 program.[45] The use of the BLYP functional has enabled a valid description of the breakage and formation of the hydrogen bonds in water,[31−33,46] poly(vinyl phosphonic acid),[36] and phosphoric acid.[35] Therefore, we are confident about the validity of the simulation results (cf. Supporting Information, Section C). The electronic wave functions were expanded in a plane wave basis set with a cutoff of 70 Ry. An empirical van der Waals correction[47] provided an inexpensive yet fairly reliable description of dispersion interactions. The correction improves the description of ab initio liquid water.[48] A time-step of 0.097 fs and a fictitious mass of 600 au were employed. The temperature was controlled by a Nosé-Hoover chain thermostat[49] with a target temperature of 310 K and a thermostat frequency of 2500 cm^{-1}. Annealing cycles and a 2 ps-long ab initio MD simulation was carried out to further equilibrate the system. The last snapshot was the initial model for two production runs. The first is a 6 ps-long ab initio MD simulation. The following properties were calculated as an average over 52 equally spaced MD snapshots: (i) The electrostatic potential $\mathbf{\Phi}$ as a function of the distance s from the channel center: $\mathbf{\Phi}(s) = (1/A)\int\int\int d^3\mathbf{r}\langle\mathbf{\Phi}(\mathbf{r})\delta(d(\mathbf{r}) - s)\rangle$ where A is the area of the interface and $d(\mathbf{r})$ is the distance of the point $\mathbf{r}$ to the channel center. $\mathbf{\Phi}(\mathbf{r}) = \sum_B(Z_B/(|\mathbf{R}_B - \mathbf{r}|) - \int d\mathbf{r}'((\rho(\mathbf{r}'))/(|\mathbf{r}' - \mathbf{r}|))$, where Z_B is the charge at nucleus B located at position $\mathbf{R}_B$ and $\rho(\mathbf{r}')$ is the electron density at position $\mathbf{r}'$, calculated on the real space grid. From $\mathbf{\Phi}(s)$ the dipole potential ΔV_{DP} is calculated as $\Delta V_{DP} = \max_s\mathbf{\Phi}(s) - \min_s\mathbf{\Phi}(s)$. (ii) The dipole moments of water molecules and of peptide groups, based on Wannier function centers.[50] The second run is an overall 11 ps-long multiple-walker metadynamics simulation,[51] where each of the 9 walkers started from a different initial position of the excess proton. This provides a qualitative estimation of the free energy profile of the excess proton as a function of a collective variable (CV) representing its distance from the channel mouth. The CV was defined similarly to the one used in the MS-EVB calculations on gA[25]

$$\frac{\sum_{i\in\{O_W\}} d_i e^{\lambda n_i}}{\sum_{i\in\{O_W\}} e^{\lambda n_i}} \quad (1)$$

where d_i is the distance between the oxygen atom i and the center of mass of the C_α backbone atoms in the residues GLY2, ALA3, ALA5, and DVA6 of the gA monomer, pointing to the center of the channel. The channel mouth is defined by the terminal group ETA16 and the following 6 residues, which together form a single turn. The set $\{O_W\}$ refers to all oxygen atoms in water or hydronium molecules and λ is a large number. n_i is the coordination number of hydrogen atoms coordinating oxygen atom i and is given by

$$n_i = \sum_{j\in\{H_W\}} \frac{1-(r_{ij}/r_c)^p}{1-(r_{ij}/r_c)^q} \quad (2)$$

where r_{ij} is the distance between oxygen atom i and hydrogen atom j with $\{H_W\}$ referring to hydrogen atoms in water or hydronium molecules. The cutoff distance r_c was set to 1.27 Å with $p = 6$ and $q = 12$.[52] Thus n_i is about 3 in case of the hydronium ion H_3O^+ and about 2 for a water molecule H_2O. The Gaussian bias potential introduced by metadynamics was deposited every 50 MD steps, initially using a height of 0.5 kcal/mol and a width of 0.25 Å, similar to refs 37 and 53. The height of the bias potential was subsequently reduced to 0.25 and 0.13 kcal/mol (cf. Supporting Information, Section D). Metadynamics trajectories were also used to calculate the proton coordination number $CN_{O^*\text{-}O}$ as in ref 54. O* refers to the oxygen atom in H_3O^+. O refers to the oxygen atoms in the water molecules and the carbonyl and hydroxyl groups of the protein. $H_5O_2^+$ ions are considered here as two resonance structures represented as H_3O^+-H_2O. The cutoff for the O*-O distance used in the calculations is 2.8 Å, as in ref [56].

RESULTS AND DISCUSSION

The maximum difference in electrostatic potential from water to the model membrane[13,17,18] (Figure 1A) calculated in our ab initio MD simulation corresponds to ΔV_{DP}. Its value is 0.40 ± 0.02 V, and it is located at the channel entrance region.[57] Our calculated value is similar to the experimental estimation of ΔV_{DP} in gA (~0.35−0.40 V) embedded in DMPC monolayers.[58]

The location of the free energy barrier identified by our ab initio metadynamics simulations appears at the channel mouth as well, coinciding with the electrostatic barrier (Figure 1A). We note, however, that the metadynamics simulation is only partially converged. Therefore, observations derived from these data should be taken as suggestions. The presence of the barrier at this location has been pointed out by experiments on gA embedded on lipid bilayers other than DMPC.[6,10−12]

Based on these observations, we suggest that the membrane dipole potential leading to a barrier at the channel mouth constitutes an important factor for the rate of proton transfer. This proposal is consistent with the experimentally observed increase of the proton permeation rate in the presence of a transmembrane voltage.[6] Indeed, if ΔV_{DP} is a key ingredient for the free energy barrier originating largely from the membrane dipole potential, then the transmembrane voltage will decrease the electrostatic potential energy of the proton along the barrier. A transmembrane potential of 0.16 V (0.06 V), such as that imposed in ref 6, would lead to about a 500-fold (10-fold) increase of the rate due to a change of the Boltzmann factor at

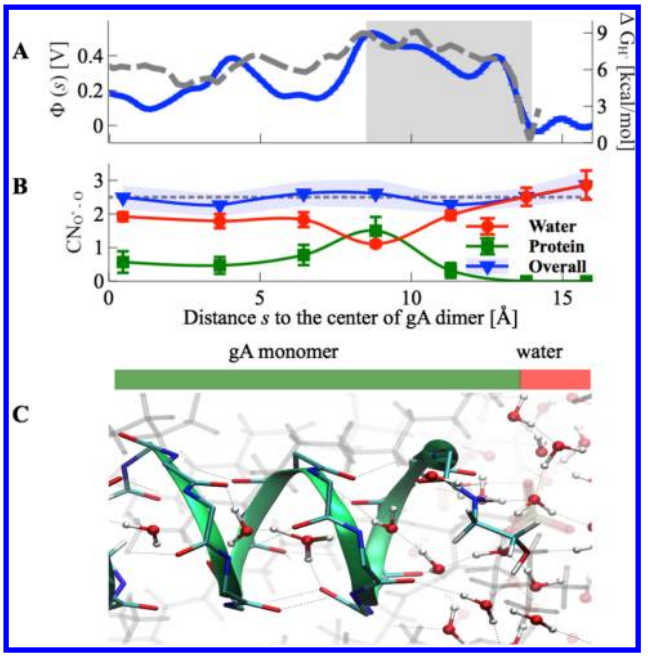

Figure 1. A: Calculated electrostatic potential of the whole system $\Phi(s)$ (blue line) and free energy profile ΔG_{H^+} (dashed gray line) for proton permeation across the gA channel as a function of the distance to the channel center. The free energy barrier is located in the shaded gray region corresponding to the channel mouth. B: Coordination number of the excess proton $CN_{O^*\text{-}O}$. Water molecule oxygen atoms, protein carbonyl/hydroxyl oxygen atoms contributions, and the overall proton coordination number are shown in red, green, and blue, respectively. C: Atomic structure of the gA channel in solvated model membrane environment, aligned with the distance scale shown in the top panel.

room temperature (see Supporting Information, Section G). This is the same order of magnitude as that observed experimentally.[6] The transmembrane potential across bacterial membranes (typically ranging from 0.06 to 0.14 V)[59] is expected to reduce the free energy barrier in vivo as well. This may play a role, at least in part, in the highly efficient proton conduction in antibiotic applications of gA.[3,4]

The water and peptide units inside the channel and at the channel mouth seem to provide an aqueous-like environment thus balancing the electrostatic destabilization upon the partial dehydration in the channel. Indeed, the water averaged dipole moments (2.8 D, Figure 2) are similar to those of pure bulk water, as measured by X-ray and neutron scattering experiments (2.9 ± 0.6 D) and to those calculated with a computational setup similar to the one used here (3.0 D).[60,61] The values spread from about 2.0 to 3.8 D (Figure 2). Similar plots are obtained for the waters and peptides (see Supporting Information, Figure S5b) in the channel mouth alone. The average peptide unit's dipole moment shows an increase on passing from the gas phase to the protein (4.4 and 6.1 D, respectively, Figure 2, see also Supporting Information for details, Figures S9 and S10 and Table S2). This is similar to the change from the gas phase to water solution calculated using ab initio MD[62] or semiempirical PM3[63] simulations (7.0 or 5.4−6.6 D, respectively) for N-methylacetamide. This finding differs from EVB calculations.[25,64] This may be caused by the fact that EVB represents electronic charge distributions only as simple sets of point charges. This point charge model cannot capture the intricate changes of waters' and peptides'

dx.doi.org/10.1021/ct400374n | J. Chem. Theory Comput. 2013, 9, 3826−3831

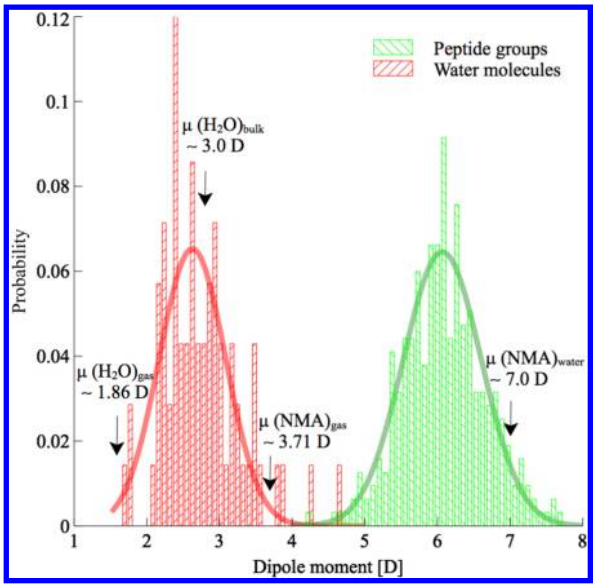

Figure 2. Distribution of the dipole moment of water molecules inside the channel and of gA's peptide units. The dipole average values are 2.8 and 6.1 D, respectively. See Supporting Information Figure S7a for a dipole moment distribution of all water molecules in the system.

electronic structure in response to a varying highly polar environment (Figures 2 and 3).

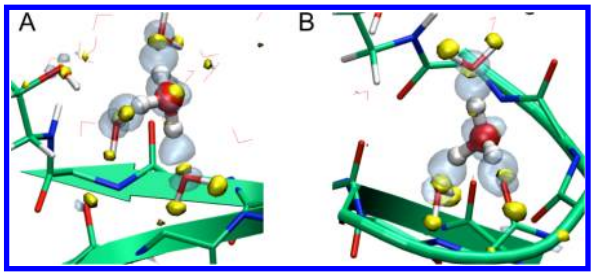

Figure 3. Electron density differences of the excess proton near the mouth of the gA channel. $\Delta\rho = \rho_{system} - \rho_{H_3O^+} - \rho_{rest}$. "System" denotes the full ab initio simulation system; "rest" refers to the rest of the system without H_3O^+. Gray transparent isosurfaces refer to positive and yellow isosurfaces denotes negative $\Delta\rho$. In this figure, the excess proton is about to enter (A) or has just entered (B) the channel.

A comparison of the coordination number of the excess proton $CN_{O^*\text{-}O}$ arising from water molecule oxygen atoms and from protein carbonyl/hydroxyl oxygen atoms contributions (Figure 1 B) suggests that at the barrier the water molecule oxygen atoms are replaced by proteins carbonyl or hydroxyl oxygen atoms in the coordination of the proton (Figure 4). The overall proton coordination number on average appears to be reduced by about 0.5 ± 0.2. Therefore, desolvation might also play a role for the entrance barrier, although convergence issues on the free energy at present do not allow us to establish this on a firm basis. Our suggestion shares some similarities with an EVB study, which provides a value of the activation free energy in agreement with experiment (Table S1).[64] Indeed, this study finds the desolvation energy of the proton playing an important role for proton permeation.

In our simulations, charge transfer effects of the proton's first and second shell ligands (the solvent and the channel's peptide carbonyl groups, Figure 3) at the channel mouth appear to be small. Integration of the electron density difference within a radius of 1 Å around atoms involved in the hydrogen bonds with the proton (Figure 2) reveals that electronic polarization and/or charge transfer effects between a pair of hydrogen-bonded donor−acceptor groups leads to a change of the charge between 0.01*e* and 0.02*e*, comparable with results found previously.[65,66] This alters the potential energy of the excess proton at the channel mouth of <1 kcal/mol as a response to the surface electrostatic potential. Charge transfer effects are thus not expected to affect the free energy barrier considerably in this case. However, the diversity in electron density differences for the proton in front of the entrance (Figure 3A) and in the mouth (Figure 3B) reveals polarization effects, the importance of which is clearly shown by the broad dipole moment distributions of the water molecules and the peptide units (Figure 2).

Representative ab initio MD snaphots of proton permeation from the bulk water through the channel entrance to the center of the gA dimer in between the two monomers connected by hydrogen bonds are shown in Figure 4. The permeation includes H_3O^+ and $H_5O_2^+$ configurations, as reported in refs 8 and 27. The H_3O^+ ion is hydrogen-bonded to three adjacent water molecules in bulk water.[67] Because of the amphiphilic character of the hydronium ion, its first coordination shell can include at most three hydrogen bond acceptors, but no hydrogen bond donor.[68,69] Inside the gA channel, these three hydrogen bond acceptors are either one channel water molecule and 2 carbonyl groups of the protein or 2 channel water molecules and 1 carbonyl group of the protein (Figure 1B). The proton obviously cannot form three hydrogen bonds with channel water molecules nor with the carbonyl groups in the protein, because of the geometrical restrains due to the single-file water molecules in the channel and the ß-helical polypeptide chain, respectively. $H_5O_2^+$ configurations are described as two water molecules connected by a shared intervening proton.[70] In such a case, each of the two water molecules again forms hydrogen bonds to the neighboring water molecules and a carbonyl group.

The sequential proton hopping between H_3O^+ and $H_5O_2^+$ configurations involves the disruption of the hydrogen bond with the carbonyl group and reorientation of the H_3O^+ ion into a favorable orientation for the subsequent transfer step.

As in any molecular simulation study, our investigation has several limitations. In our case, these include the relatively small size of the simulated system since electrostatic interactions between the central box and nearby periodic replicas may affect the results. However, we notice a posteriori that the calculated membrane dipole potential is in rather good accord with previous experimental works.[11,12,58] Another limitation is the accuracy of the potential energy surface generated by our BLYP calculations[55] despite the presence of corrections for van der Waals interactions.[47] Nuclear quantum effects (not included here) are expected to be small in this specific case.[31] Furthermore, the specificity of the membrane type for ΔV_{DP} as well as proton transfer energetics, emerging from MS-EVB studies,[25] is not addressed here.

Arguably, the most important limitation is due to sampling issues. In particular, our short metadynamics simulations can at most provide suggestions on the role of desolvation and the location of the free energy barrier. Longer and more converged calculations are required to establish those as well as to estimate $\Delta G^{\#}$ quantitatively.

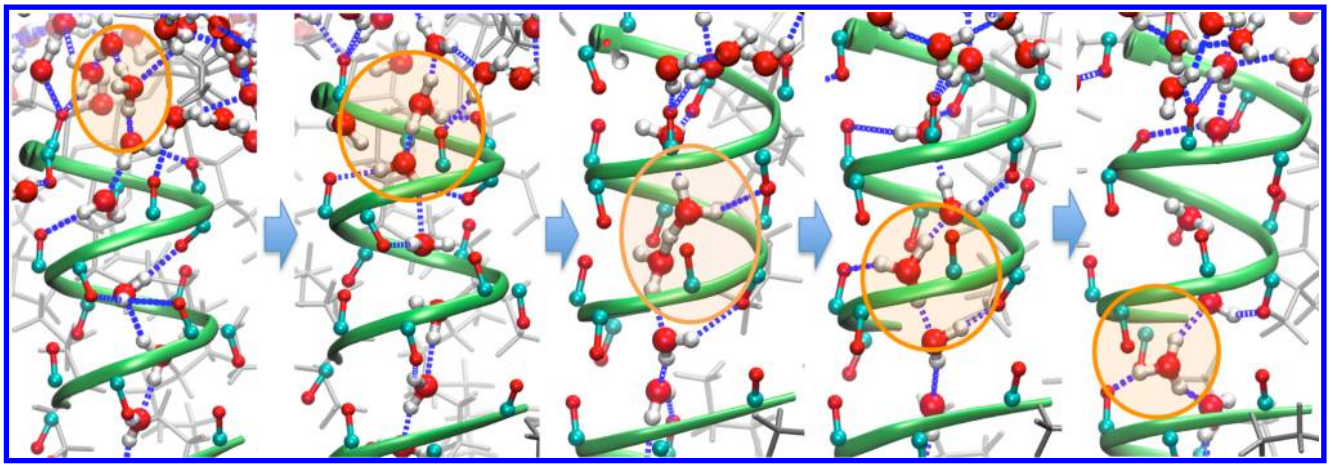

Figure 4. Representative structures for proton conduction from bulk water (left) through the entrance of the gA channel to the center in between the two monomers (right). Structures represent H_3O^+ and $H_5O_2^+$ configurations, hydrogen-bonded (blue dashed lines) to adjacent water molecules as well as to peptide carbonyl groups. The protein ß-helix is sketched in green; the lipid molecules are represented in gray. Water molecules and peptide C═O groups are shown in CPK representation.

CONCLUSIONS

This work provides insights on the role of the membrane dipole potential for proton permeation in gA in the DMPC bilayer. It suggests that the free energy barrier is located at the channel's mouth. These findings are consistent with the available experimental data measured for gA in DMPC monolayers[58] and other membrane bilayers including GMO and DPhPC.[6,10−12] They may also explain why the rate of proton conduction increases dramatically in the presence of a transmembrane potential.

ASSOCIATED CONTENT

Supporting Information

List of reported free energy barriers of proton permeation in the gramicidin A channel; Setup of the system with classical MD simulations; Accuracy of density functional theory for ab initio molecular dynamics of water and proton permeation; Choice of parameters for ab initio metadynamics simulations; Validations of protein structure in ab initio simulations; Convergence of the calculated electrostatic potential; Influence of the transmembrane potential on reaction rates; Dipole moment distributions; Water molecule orientations along the channel *z*-axis; Dipole moments for local peptide groups; Previous EVB and MS-EVB calculations. This material is available free of charge via the Internet at http://pubs.acs.org.

AUTHOR INFORMATION

Corresponding Author

*E-mail: p.carloni@grs-sim.de (P.C.), j.dreyer@grs-sim.de (J. D.).

Present Address

[#]Johannes Gutenberg University Mainz, Institute of Physics Chemistry and Center for Computational Studies, Staudinger-weg 7, D- 55129, Mainz, Germany.

Author Contributions

J.D. ran the calculations. C.Z. and P.C. conceived the project and contributed to the scientific discussion. E.I. participated to the discussions. All of the authors wrote the manuscript.

Notes

The authors declare no competing financial interest.

ACKNOWLEDGMENTS

We gratefully acknowledge that this work has been achieved using the PRACE (http://www.praceproject.eu) research infrastructure resource JUGENE hosted by Forschungszentrum Jülich in Germany.

ABBREVIATIONS

BLYP, Becke exchange functional with Lee−Yang−Parr correlation functional; CPMD, Car−Parrinello molecular dynamics; DFT, density functional theory; DMPC, 1,2-dimyristoyl-sn-glycero-3-phosphocholine; DOPC, dioleoyl-phosphatidylcholine; DPhPC, diphytanoylphosphatidylcholine; DPPC, dipalmitoylphosphatidylcholine; (MS-) EVB, (multi state-) empirical valence bond; gA, gramicidin A; GMO, glycerol 1-monooleate; MD, molecular dynamics; NMR, nuclear magnetic resonance

REFERENCES

(1) Van Epps, H. L.; Dubos, R. *J. Exp. Med.* **2006**, *203*, 259.
(2) Patton, T. G.; Yang, S. J.; Bayles, K. W. *Mol. Microbiol.* **2006**, *59*, 1395−1404.
(3) Matsui, R.; Cvitkovitch, D. *Future Microbiol.* **2010**, *5*, 403−417.
(4) Thibodeau, E. A.; Marquis, R. E. *J. Dent. Res.* **1983**, *62*, 1174−1178.
(5) Dashper, S. G.; Reynolds, E. C. *J. Dent. Res.* **1992**, *71*, 1159−1165.
(6) Cukierman, S. *Biophys. J.* **2000**, *78*, 1825−1834.
(7) Chernyshev, A.; Pomès, R.; Cukierman, S. *Biophys. Chem.* **2003**, *103*, 179−190.
(8) Pomès, R.; Roux, B. *Biophys. J.* **2002**, *82*, 2304.
(9) Woolley, A. G.; Wallace, B. *J. Membr. Biol.* **1992**, *129*, 109−136.
(10) Decoursey, T. E. *Physiol. Rev.* **2003**, *83*, 475−579.
(11) Chernyshev, A.; Cukierman, S. *Biophys. J.* **2002**, *82*, 182−192.
(12) Chernyshev, A.; Cukierman, S. *Biophys. J.* **2006**, *91*, 580−587.
(13) Wang, L. *Annu. Rev. Biochem.* **2012**, *81*, 615−635.
(14) Rokitskaya, T. I.; Kotova, E. A.; Antonenko, Y. N. *Biophys. J.* **2002**, *82*, 865−873.
(15) Marcelo, G.; de Godoy, C.; Cukierman, S. *Biophys. J.* **2001**, *81*, 1430−1438.
(16) Harder, E.; MacKerell, A. D.; Roux, B. *J. Am. Chem. Soc.* **2009**, *131*, 2760−2761.
(17) Pohl, P.; Rokitskaya, T. I.; Pohl, E. E.; Saparov, S. M. *Biochim. Biophys. Acta, Biomembr.* **1997**, *1323*, 163−172.

(18) Peterson, U.; Mannock, D. A.; Lewis, R. N. A. H.; Pohl, P.; McElhaney, R. N.; Pohl, E. E. *Chem. Phys. Lipids* **2002**, *117*, 19−27.
(19) Yang, Y.; Mayer, K. M.; Wickremasinghe, N. S.; Hafner, J. H. *Biophys. J.* **2008**, *95*, 5193−5199.
(20) Disalvo, E. A.; Lairion, F.; Martini, F.; Tymczyszyn, E.; Frías, M.; Almaleck, H.; Gordillo, G. J. *Biochim. Biophys. Acta, Biomembr.* **2008**, *1778*, 2655−2670.
(21) Kathmann, S. M.; Kuo, I.-F. W.; Mundy, C. J.; Schenter, G. K. *J. Phys. Chem B* **2011**, *115*, 4369−4377.
(22) *At this high H^+ concentration, phospholipids may become increasingly screened by adsorbing H^+ and anions at the interface. As expected, this affects dramatically ΔV_S.*[13]
(23) Quigley, E. P.; Quigley, P.; Crumrine, D. S.; Cukierman, S. *Biophys. J.* **1999**, *77*, 2479−2491.
(24) Cukierman, S.; Quigley, E. P.; Crumrine, D. S. *Biophys. J.* **1997**, *73*, 2489−2502.
(25) Qin, Z.; Tepper, H. L.; Voth, G. A. *J. Phys. Chem B* **2007**, *111*, 9931−9939.
(26) Car, R.; Parrinello, M. *Phys. Rev. Lett.* **1985**, *55*, 2471−2474.
(27) Sagnella, D. E.; Laasonen, K.; Klein, M. L. *Biophys. J.* **1996**, *71*, 1172−1178.
(28) Marx, D.; Tuckerman, M.; Hutter, J.; Parrinello, M. *Nature* **1999**, *397*, 601−604.
(29) Tuckerman, M. E.; Marx, D.; Parrinello, M. *Nature* **2002**, *417*, 925−929.
(30) Izvekov, S.; Voth, G. A. *J. Chem. Phys.* **2005**, *123*, 044505.
(31) Tuckerman, M. E.; Chandra, A.; Marx, D. *Acc. Chem. Res.* **2006**, *39*, 151−158.
(32) Berkelbach, T. C.; Tuckerman, M. E. *Phys. Rev. Lett.* **2009**, *103*, 238302.
(33) Marx, D.; Chandra, A.; Tuckerman, M. E. *Chem. Rev.* **2010**, *110*, 2174−2216.
(34) Hayes, R. L.; Paddison, S. J.; Tuckerman, M. E. *J. Phys. Chem. A* **2011**, *115*, 6112−6124.
(35) Vilčiauskas, L.; Tuckerman, M. E.; Bester, G.; Paddison, S. J.; Kreuer, K.-D. *Nat. Chem.* **2012**, *4*, 461−466.
(36) Ludueña, G. A.; Kühne, T. D.; Sebastiani, D. *Chem. Mater.* **2011**, *23*, 1424−1429.
(37) Zhang, C.; Knyazev, D. G.; Vereshaga, Y. A.; Ippoliti, E.; Nguyen, T. H.; Carloni, P.; Pohl, P. *Proc. Natl. Acad. Sci. U.S.A.* **2012**, *109*, 9744−9749.
(38) Jensen, M. Ø.; Röthlisberger, U.; Rovira, C. *Biophys. J.* **2005**, *89*, 1744−1759.
(39) Rousseau, R.; Kleinschmidt, V.; Schmitt, U. W.; Marx, D. *Angew. Chem., Int. Ed.* **2004**, *43*, 4804−4807.
(40) Mathias, G.; Marx, D. *Proc. Natl. Acad. Sci. U.S.A.* **2007**, *104*, 6980−6985.
(41) Laio, A.; VandeVondele, J.; Rothlisberger, U. *J. Chem. Phys.* **2002**, *116*, 6941−6947.
(42) Ketchem, R. R.; Lee, K. C.; Huo, S.; Cross, T. A. *J. Biomol. NMR* **1996**, *8*, 1−14.
(43) Gowen, J. A.; Markham, J. C.; Morrison, S. E.; Cross, T. A.; Busath, D. D.; Mapes, E. J.; Schumaker, M. F. *Biophys. J.* **2002**, *83*, 880−898.
(44) Chattopadhyay, A.; Rawat, S. S.; Greathouse, D. V.; Kelkar, D. A.; Koeppe, R. E. *Biophys. J.* **2008**, *95*, 166.
(45) *CPMD*, Copyright IBM Corp 1990−2008, Copyright MPI für Festkörperforschung Stuttgart 1997−2001. http://www.cpmd.org/ (accessed June 12, 2013).
(46) Tuckerman, M. E.; Chandra, A.; Marx, D. *J. Chem. Phys.* **2010**, *133*, 124108.
(47) Grimme, S. *J. Comput. Chem.* **2004**, *25*, 1463−1473.
(48) Schmidt, J.; VandeVondele, J.; Kuo, I. F. W.; Sebastiani, D.; Siepmann, J. I.; Hutter, J.; Mundy, C. J. *J. Phys. Chem. B* **2009**, *113*, 11959−11964.
(49) Martyna, G. J.; Klein, M. L.; Tuckerman, M. E. *J. Chem. Phys.* **1992**, *97*, 2635−2643.
(50) Marzari, N.; Vanderbilt, D. *Phys. Rev. B* **1997**, *56*, 12847−12865.
(51) Raiteri, P.; Laio, A.; Gervasio, F. L.; Micheletti, C.; Parrinello, M. *J. Phys. Chem. B* **2006**, *110*, 3533−3539.
(52) Park, J. M.; Laio, A.; Iannuzzi, M.; Parrinello, M. *J. Am. Chem. Soc.* **2006**, *128*, 11318−11319.
(53) Ensing, B.; Klein, M. L. *Proc. Natl. Acad. Sci. U.S.A.* **2005**, *102*, 6755−6759.
(54) Wu, Y.; Hanning, C.; Wang, F.; Paesani, F.; Voth, G. A. *J. Phys. Chem. B* **2008**, *112*, 467.
(55) Geissler, P. L.; Voorhis, T. V.; Dellago, C. *Chem. Phys. Lett.* **2000**, *324*, 149−155.
(56) Brancato, G.; Tuckerman, M. E. *J. Chem. Phys.* **2005**, *122*, 224507−224511.
(57) Cf. Figure S4 *for the running average of the electrostatic potential showing its convergence with an increasing number of averaged snapshots.*
(58) Shapovalov, V. L.; Kotova, E. A.; Rokitskaya, T. I.; Antonenko, Y. N. *Biophys. J.* **1999**, *77*, 299−305.
(59) Jack, R. W.; Tagg, J. R.; Ray, B. *Microbiol. Rev.* **1995**, *59*, 171−200.
(60) Silvestrelli, P. L.; Parrinello, M. *Phys. Rev. Lett.* **1999**, *82*, 3308−3311.
(61) Morrone, J. A.; Car, R. *Phys. Rev. Lett.* **2008**, *101*, 017801.
(62) Gaigeot, M. P.; Vuilleumier, R.; Sprik, M.; Borgis, D. *J. Chem. Theory Comput.* **2005**, *1*, 772−789.
(63) Ingrosso, F.; Monard, G.; Hamdi Farag, M.; Bastida, A.; Ruiz-López, M. F. *J. Chem. Theory Comput.* **2011**, *7*, 1840−1849.
(64) Braun-Sand, S.; Burykin, A.; Chu, Z. T.; Warshel, A. *J. Phys. Chem. B* **2005**, *109*, 583−592.
(65) Fonseca Guerra, C.; Bickelhaupt, F. M.; Snijders, J. G.; Baerends, E. J. *J. Am. Chem. Soc.* **2000**, *122*, 4117−4128.
(66) Bucher, D.; Raugei, S.; Guidoni, L.; Peraro, M. D.; Rothlisberger, U.; Carloni, P.; Klein, M. L. *Biophys. J.* **2006**, *124*, 292−301.
(67) Eigen, M. *Angew. Chem., Int. Ed.* **1964**, *3*, 1−19.
(68) Petersen, M. K.; Iyengar, S. S.; Day, T. J. F.; Voth, G. A. *J. Phys. Chem. B* **2004**, *108*, 14804−14806.
(69) Kudin, K. N.; Car, R. *J. Am. Chem. Soc.* **2008**, *130*, 3915−3919.
(70) Zundel, G. *Adv. Chem. Phys.* **2000**, *111*, 1−217.